New Insights into the Formation Mechanism of Intertwining Interfaces in Cold Spray

Shuo Yin, Rocco Lupoi

a. Trinity College Dublin, The University of Dublin, Department of Mechanical and Manufacturing Engineering, Parsons Building, Dublin 2, Ireland

yins@tcd.ie, lupoir@tcd.ie

Jan Cizek

b. Institute of Plasma Physics, Czech Academy of Sciences, Za Slovankou 1782/3, 182 00 Prague, Czech Republic

Abstract

Experimental investigation supported by numerical modeling was conducted to explore the formation mechanism of intertwining interface in cold spray. The result revealed that low particle impact velocity and the consequent low deposition efficiency were the essential reason for inducing intertwining interface. In addition, intertwining interface was found to generate at very beginning of coating deposition; further particle deposition posed negligible effect on the formation of intertwining interface. Based on the experimental and numerical analysis, for the first time, the formation mechanism of intertwining interface was concluded and proposed in this paper. Low deposition efficiency led to slow coating growing rate. Therefore, at the beginning of the coating deposition, a large number of rebound particles repetitively hit the very thin single-layer or double-layer coating, forming a shot-peening effect. Such effect resulted in periodic shear stress and plastic strain in the first-layer coating. Particles of the first-layer coating were elongated and fractured and mixed with the substrate material to form the intertwining structure.

Introduction

Cold spray is a low-temperature coating and additive manufacturing technology developed in the 1980s [1]. Feedstock powders are accelerated by the supersonic propellant gas in a Laval nozzle and subsequently impact onto a substrate. If the particle impact velocity exceeds a so-called 'critical velocity', coatings or bulk deposits can be formed on the substrate surface without exceeding their melting points [2,3]. Therefore, defects encountered in the related high-temperature deposition processes, such as oxidation, thermal residual stress and phase transformation, can be effectively avoided [4–8]. Due to the above mentioned merits, cold spray has been regarded as a promising coating and additive manufacturing technology, attracting great attention from both scientific and industrial communities in recent years.

Despite cold spray can be used to deposit many different materials, metals coated onto metals are still the most popular cases which have been intensively investigated. In this respect, bonding mechanism of metals in contact is always a major research focal point. A number of works have been carried out during the past decades to improve our understanding on this issue [4,5,7]. It has been well recognized that metallurgical bonding and mechanical interlocking are two dominant mechanisms of metallic bonding in cold spray. Metallurgical bonding is known to result from nano-scale chemical reaction at the inter-particle or coating-substrate interfaces [6,9–14]. Mechanical interlocking, as another important mechanism, contributes only to coating-substrate adherence. It is commonly present in cases where the substrate material is softer than the particle material. As a non-chemical bonding, the interlocking is represented by hard particle material mechanically embedded into and trapped by the soft substrate material [15,16]. Overall, after investigation for years, most of the important issues in regard to the metallurgical bonding and mechanical interlocking have been understood so far.

However, apart from the two major bonding mechanisms, another important bonding phenomenon in the form of particle fracture and mutual intertwining at the coating-substrate interface was observed in very rare cases when hard coatings were deposited onto soft substrates [17–19]. Currently, no studies have inquired into the fundamental principles of such intertwining interface as yet. Thereby, its inducing conditions and formation mechanism are still not well understood. In this work, for the first time, a targeted experimental study with copper onto aluminum substrate was conducted, supported by numerical modeling, to clarify the substantial formation mechanism and inducing conditions of the intertwining interface.

Experimental methodology

Coating fabrication

Spherical copper powders (-38+15 mm, > 99.9%, Safina, Czech Republic) were selected as the feedstock. Fig. 1 shows the surface morphology of the copper powders observed by SEM (Carl Zeiss Ultra Plus, Germany). Soft aluminum sheets with polished flat surface were used as the substrates. The cold sprayed copper coatings were fabricated using a self-made CS system (Trinity College Dublin, Ireland) [20]. The Lavel nozzle used in this work has a round shape with a divergent length of 180 mm, a throat of 2mm and an outlet diameter of 6 mm. Standoff distance (SOD) between the nozzle exit and

substrate was set as 30 mm. Compressed nitrogen with a constant pressure of 2.5 MPa was used as the propellant gas. Single-track coating was produced for all trails to eliminate the potential effect of spraying strategy on the coating deposition process. Propellant gas temperature (100, 150, 200 and 300 ° C), number of nozzle passes (2, 4, 6 and 8) and nozzle moving speed (25, 50, 100 mm/s) varied to produce coatings with different features. Detailed deposition conditions of the produced coatings are provided in Table 1.

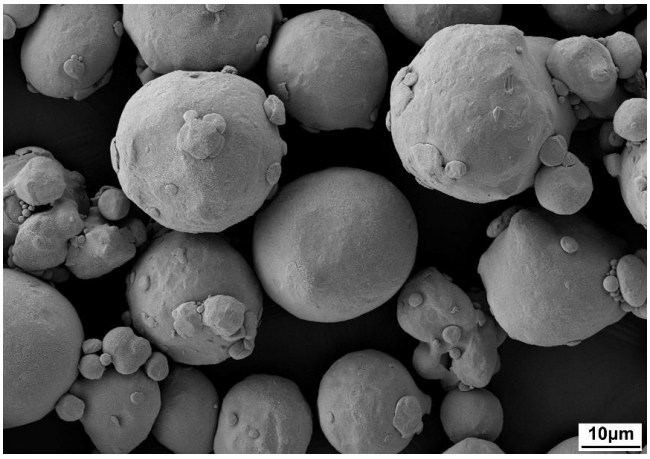

Figure 1: Surface morphology of the copper powders used in this work

Table 1. Deposition conditions of the produced coatings

Temperature, °C	Nozzle pass	Nozzle speed, mm/s
100	4	50
150	4	50
200	4	50
300	4	50
150	**2**	50
150	**4**	50
150	**6**	50
150	**8**	50
150	4	**25**
150	4	**50**
150	4	**100**

Materials characterization

The microstructure of the cold sprayed coating and substrate materials at the interface was studied by SEM in secondary electrons mode. To assess the coating microstructure via SEM, the as-sprayed coating samples were cut along the longitudinal direction for the coating-substrate interface observation and horizontal direction for the overall coating shape observation, respectively. The as-cut samples were then prepared using standard metallographic procedures with the final polishing applied by 0.06 μm silica solution. For all trails, coating thickness was measured to evaluate the coating deposition efficiency under different working parameters.

Numerical methodology

Model design

For assisting the experimental investigation, numerical simulation was performed to study the plastic deformation at the first-layer coating and coating-substrate interfacial region during the coating deposition. A well-designed coating deposition model as illustrated in Fig. 2 was proposed in this work to achieve this objective. As shown in the schematic, the cold sprayed coating is represented by many single layers, where single layer is defined as the coating formed with only one-layer particles. This work only concerned the potential plastic deformation of the first-layer coating and coating-substrate interfacial region. In addition, considering the flattening of the particles after deposition, each layer was given a thickness of 13 μm, which is half of the particle average diameter.

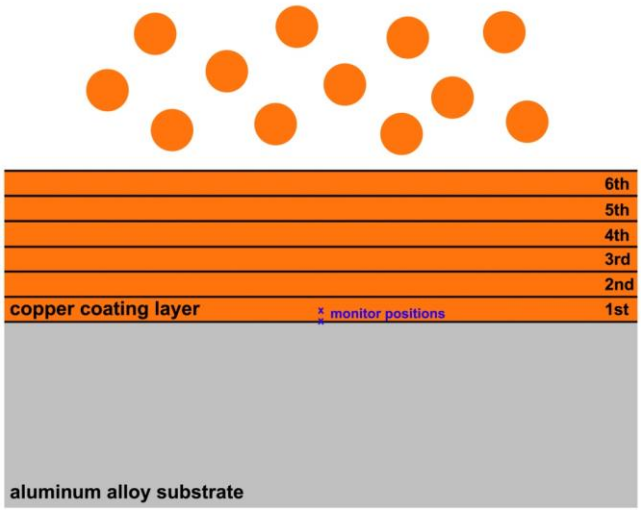

Figure 2: Schematic of the coating deposition model used in the simulation. Monitor positions were highlighted with blue cross

Numerical model description

Numerical simulation was performed using a commercial software, ABAQUS. Lagrangian algorithm with the dynamic explicit procedure was applied to build the computational model. Copper particle was defined as a sphere with the diameter of 26 μm (i.e., same as in the experiment), while aluminum substrate was defined as a cylinder with a diameter and height of 260 and 130 μm, respectively. Because of symmetric nature of the impact process, the computational model was simplified as 2D axisymmetric model in order to reduce the computational time. The contact process was implemented by using the surface-to-surface penalty contact algorithm with balanced contact pair formulation. The fixed boundary condition was enforced to the substrate bottom and lateral surfaces. The geometry was partitioned by the four-node bilinear axisymmetric quadrilateral elements with

reduced integration and hourglass control (CAX4R). Fig. 3 shows the local computational domain and meshing of the used computational model. Three monitor elements were selected at the intertwining interface. Monitor element 1 is located at the central point of the first-layer coating where fracture took place as revealed by the experiment. Monitor element 2 and 3 represent the coating-substrate interface. The particle impact velocity was defined as between 200 and 500 m/s based on the simulated results by Ansys-Fluent according to the experimental conditions.

The metal materials were described by the Johnson and Cook (JC) plasticity model, which accounts for strain and strain-rate hardening, as well as thermal softening [21]. Detailed parameters for JC mode can be found elsewhere [22].

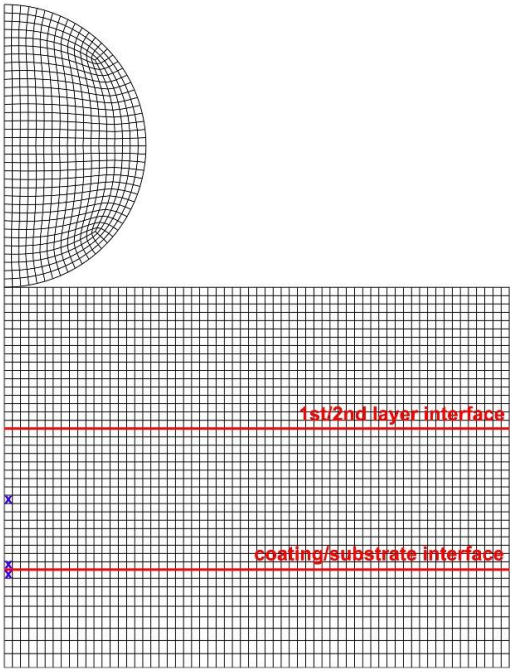

Figure 3: Local computational domain, meshing and three selected monitor elements of the numerical model. Monitor elements were highlighted with blue cross

Results and discussion

Coating thickness and deposition efficiency

Fig. 4 shows the measured overall coating thickness as function of gas temperature, number of nozzle passes and nozzle moving speed. It is clearly seen that the overall coating thickness went up dramatically with increasing the gas temperature due to the increased particle impact velocity at higher gas temperature that enhanced the coating deposition efficiency [23]. In addition, as the number of nozzle passes increased or the nozzle moving speed decreased, the coating thickness also exhibited an increasing trend. The reason for the thickness increment in these two cases was different from the former case. Here, the particle impact velocity and the consequent coating deposition efficiency were roughly the same in all trails; the thickness increment was actually caused by the longer deposition time rather than higher particle impact velocity

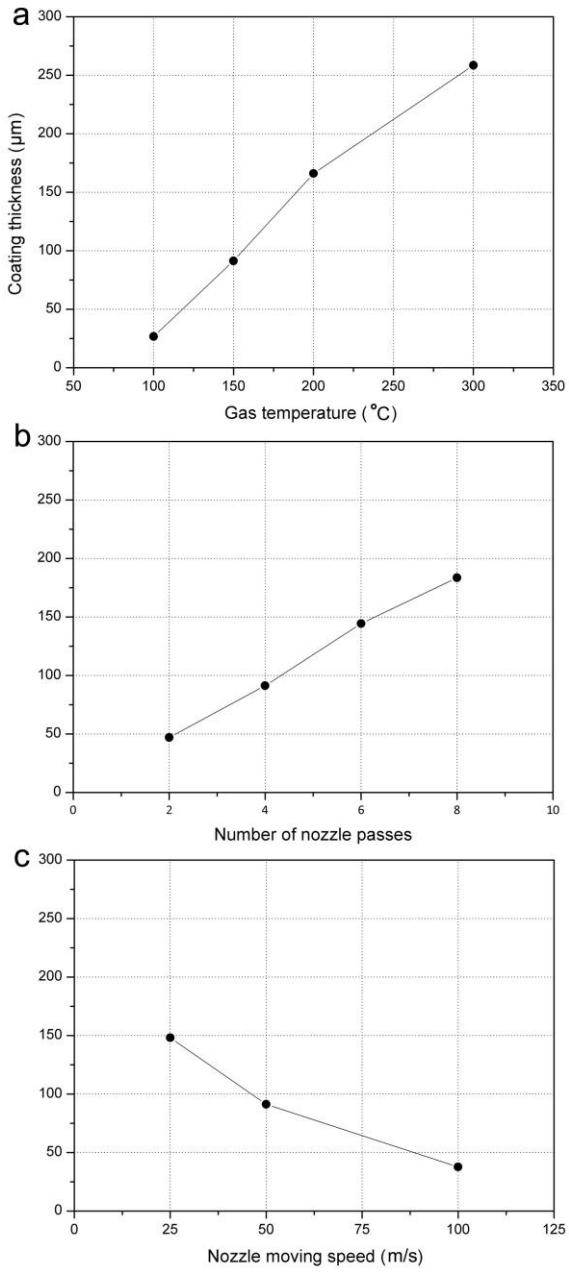

Figure 4: Coating thickness as function of gas temperature, number of nozzle passes and nozzle moving speed

Coating-substrate interface

Fig. 5 shows the cross-sectional images of the coating-substrate interfaces produced at different gas temperatures. It is interesting to find that the interfaces exhibited significantly different features as the gas temperature increased. At low gas temperature as shown in Fig. 5a and 5b, the interfaces were characterized by the strong mutual intertwining structure. As the gas temperature increased to 200 °C, intertwining phenomenon significantly weakened, being hard to observe along the interface. When the gas temperature was further increased to 300 °C, intertwining phenomenon completely vanished along the entire interface. The variation of the

interfacial features with the gas temperature clearly suggests that intertwining interface only occurred at low gas temperature. As discussed in the last section, gas temperature affected both the coating deposition efficiency and overall coating thickness through the particle impact velocity. Therefore, it is sensible that the inducing conditions of the intertwining interface is linked to either the low coating deposition efficiency or the overall coating thickness or both. In order to further clarify the inducing conditions, Fig. 6 and Fig. 7 show the cross-sectional images of the coating-substrate interfaces at different nozzle passes and moving speeds. Note that the gas temperature for these trails was set at a low level (150 °C) at which intertwining phenomenon can take place. As can be seen, all of the interfaces demonstrated similar intertwining phenomenon regardless of the overall coating thickness. This fact indicates that the intertwining interface was truly present at low gas temperature and irrelevant with the overall coating thickness. Therefore, from the experimental results shown in Fig. 5-7, it can be concluded that the intertwining interface was not affected by the overall coating thickness but only be the coating deposition efficiency. In other words, the inducing condition for intertwining interface were low coating deposition efficiency or low particle impact velocity. Furthermore, the increment of the number of nozzle passes can be roughly considered as the coating growing process. In Fig. 6, the intertwining interface had no significant change as the number of nozzle passes increased from two to eight. This fact demonstrates that the formation of intertwining interface may happen at the very beginning of the coating deposition; further particle deposition (or further coating deposition) posed negligible effect.

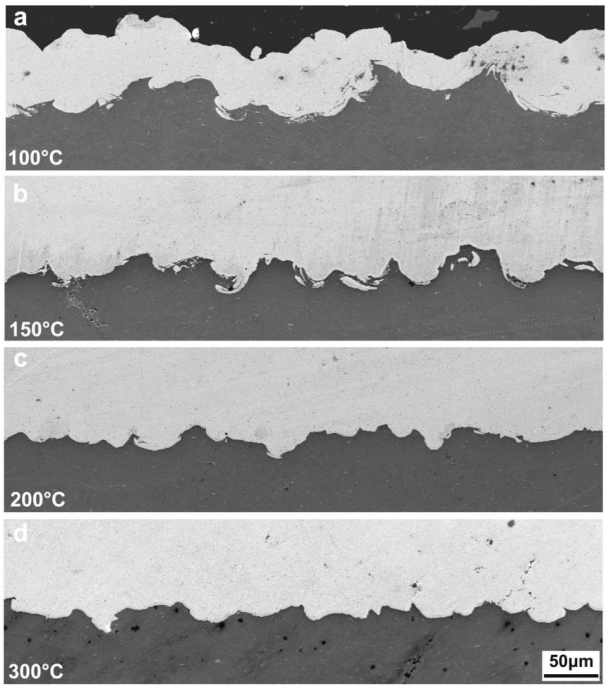

Figure 5: Cross-sectional SEM images of coating-substrate interfaces at different gas temperatures

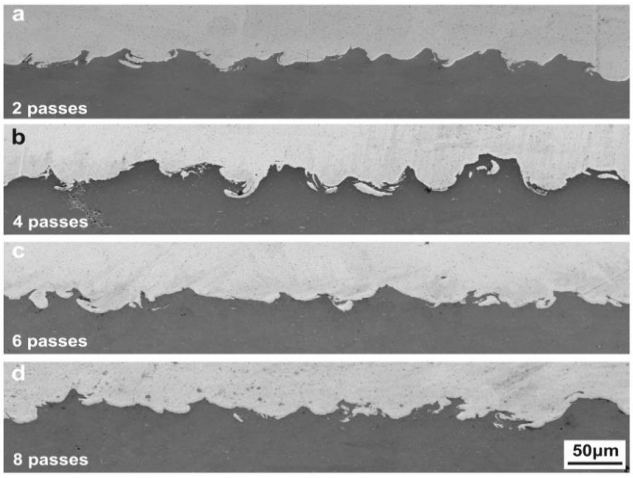

Figure 6: Cross-sectional SEM images of coating-substrate interfaces at different nozzle passes

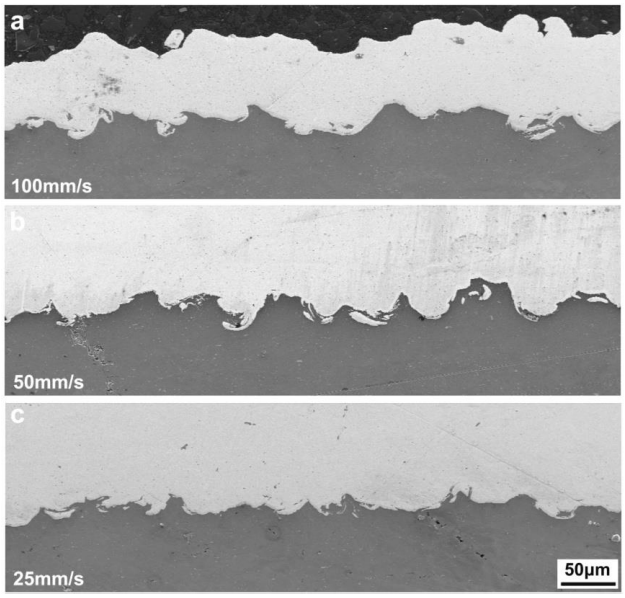

Figure 7: Cross-sectional SEM images of coating-substrate interfaces at different nozzle moving speed

Microstructure at the intertwining interface

Fig. 8 provides some typical microstructures at the intertwining interface. In Fig. 8a, the coating-substrate interface was selected from the outer zone of the coatings produced at the gas temperature of 100°C. Due to the lower deposition efficiency at the outer zone than the central zone [24,25], the coating shown in Fig. 8a consisted of only one layer. Apparently, strong intertwining structures were observed beneath the single-layer coating. This fact further confirms that intertwining interface is formed at the beginning of the coating deposition. Fig. 8b shows a single copper particle selected from the same zone as in the Fig. 8a. As can be seen, copper material at the right side was significantly elongated, while seriously deformed copper material was fractured and covered by the aluminum substrate material at the left side. Additionally, a large open crack generated at the lower part of the particle. As discussed above, the deposition efficiency at

the gas temperature of 100°C was rather low, which means that a large number of particles will rebound rather than deposition after impact. These rebound particles repetitively hit the deposited particle, leading to a shot-peening effect. Such effect resulted in periodic shear stress and plastic strain in the first-layer coating, which significantly elongated and fractured the particles. It also led to the plastic deformation of substrate material that enlarged the cracks and caused the movement of particle fragments. In addition, these rebound particles may hit the convex aluminum substrate material to induce the copper-inclusion structure as shown in Fig. 8a. Fig. 8b shows a high-magnification view of a slim crack in the copper particle. It is sensible that if the substrate material plastic deformation is larger, this slim crack will finally become the large open crack as similar to in Fig. 8b. Fig. 8d shows a single copper particle selected from coatings produced at the gas temperature of 150°C. In this case, copper fracture phenomenon and intertwining structure were still prominent. In addition to the open cracks, some inner cracks were also formed in the particle.

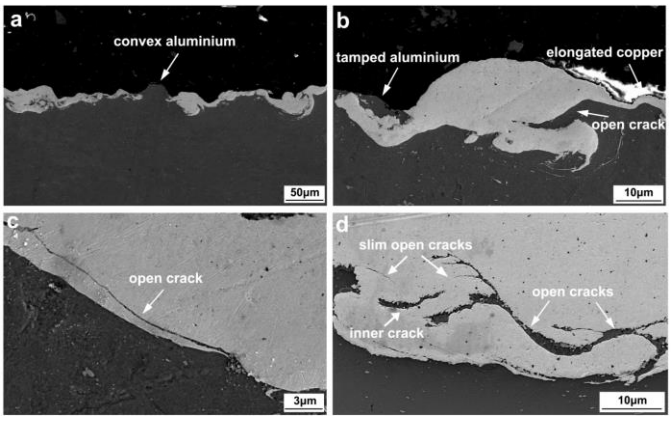

Figure 8: Typical microstructures at the intertwining interface

Plastic deformation at the intertwining interface

From the above experimental observation, it is find that intertwining interface is a consequence of plastic deformation of both particles and substrate during the coating deposition. Therefore, in order to deeply analyze the plastic deformation behavior at the intertwining interface, Fig. 9 shows the simulated PEEQ at three monitor elements against the number of coating layers. Clearly, the impact of the cold sprayed particles caused plastic deformation at the intertwining interface. However, strong plastic strain only happened in the case of single-layer and double-layer coatings. When the coating exceeds two layers, PEEQ at the monitor elements reduced dramatically and even came to zero regardless of the impact velocity. This fact suggests that the impact-induced plastic deformation at the intertwining interface was triggered only when the number of coating layers was low. The result well explains why intertwining interface generated at the beginning of the coating deposition as revealed by the experiment (because single- or double-layer coating only formed at the beginning).

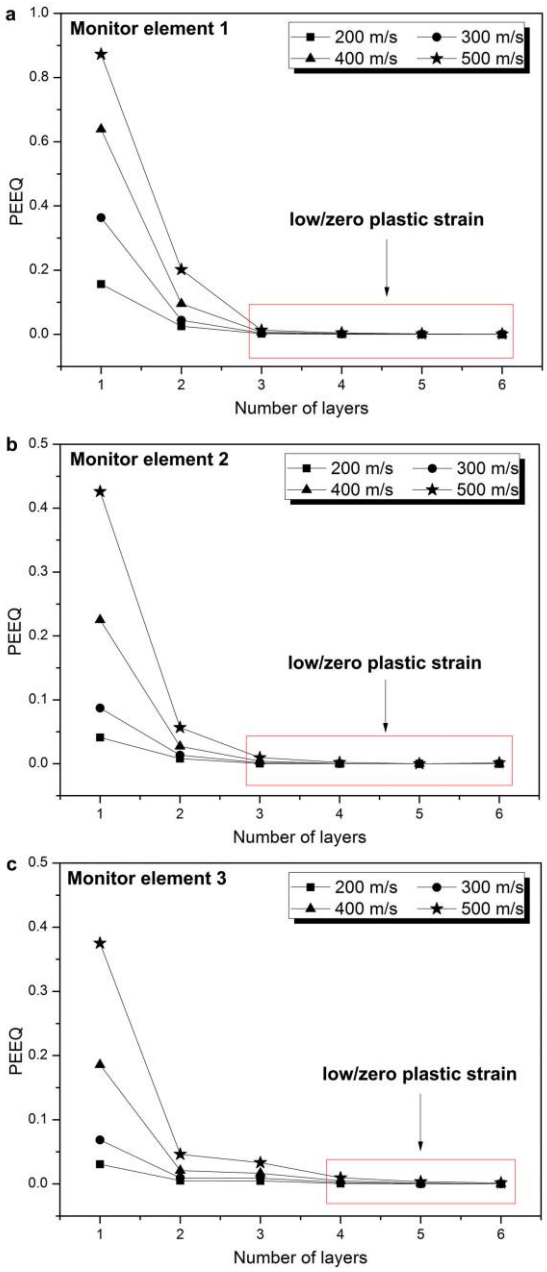

Figure 9: PEEQ against number of coating layers at three monitor elements

In addition, it is also found from Fig. 9 that, even low particle impact velocity in the case of single- and double-layer coatings would result in much higher plastic deformation at the intertwining interface than high particle impact velocity in the case of thick-layer coatings. This fact suggests that, despite lower impact velocity provided lower impact energy, the thinner-layer coating and a larger number rebound particles as a result of the lower coating growing rate can cause much stronger peening effect on the intertwining interface, explaining why intertwining interface only generated at low impact velocity. Moreover, PEEQ at the central point of the single-layer coating is much higher than at the coating-substrate interface. This is the reason why copper particles underwent fracture but substrate material only experienced limited plastic deformation.

The variation of PEEQ against the number of coating layers can be well explained through the energy analysis. During the particle deposition process, the initial particle kinetic energy is mainly dissipated through the plastic deformation of particles, deposited coating and substrate [3,26], which can be expressed as follows,

$$E=Ep+Ec+Es \quad \text{Eq. 1}$$

where E is the total plastic dissipation energy, Ep is the particle plastic dissipation energy, Ec is the coating plastic dissipation energy and Es is the substrate plastic dissipation energy. In order to analysis the plastic dissipation energy of the first-layer coating, Ec is further expressed by Ec=Ec1+Ecr, where Ec represents the first-layer coating, Ecr represents the rest of the coating. In this case, the total plastic dissipation energy, E, can be expressed as follow,

$$E=Ep+Ec1+Ecr+Es \quad \text{Eq. 2}$$

Fig. 10 show the energy dissipated through the plastic deformation of first-layer coating (Ec1) and substrate (Es). Clearly, the plastic dissipation energy for the first-layer coating and substrate significantly reduced as the number of coating layers increased from one to three, which is consistent with the variation trend of PEEQ as shown in Fig. 9. The energy analysis further reveals the plastic deformation behavior at the intertwining interface during the coating deposition.

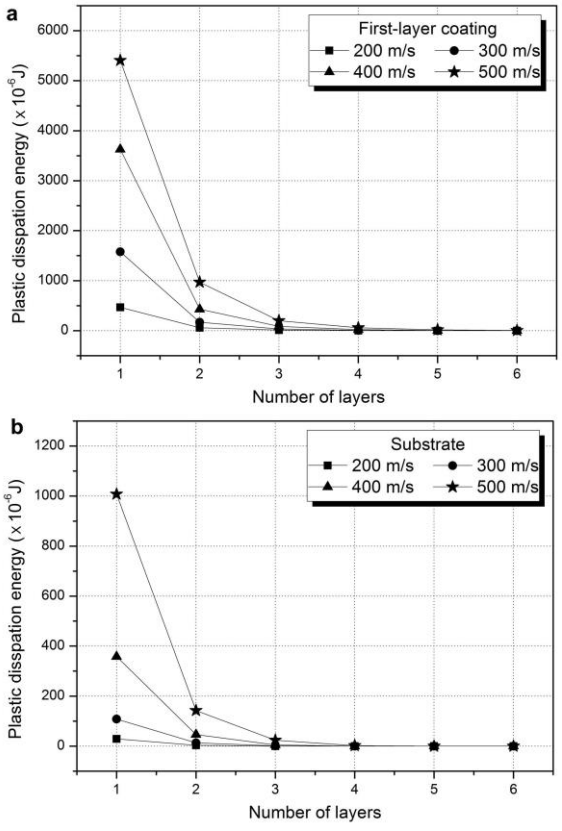

Figure 10: Energy dissipated through the plastic deformation of first-layer particles and substrate

Formation mechanism of intertwining interface

Based on the above experimental and numerical analysis, the formation mechanism of intertwining interface in cold spray was discussed and proposed in this section. First of all, it has been concluded from Fig. 5-7 that intertwining interface only generated at low deposition efficiency (or low particle impact velocity). On one hand, low deposition efficiency results in very slow coating growing rate, which means that the coating thickness will maintain at a low level for a long time. According to the simulation result, only for the thin-layer coating will the interfacial region experience high plastic deformation upon the impact by the cold sprayed particles. On the other hand, lower deposition efficiency simultaneously results in a larger number of rebound particles as shown in Fig. 11a. These rebound particles repetitively hit the thin-layer coating, periodically inducing plastic strain of the first-layer particles and interfacial materials. Then, after peening for numerous times, fracture takes place in the first-layer coating, breaking the copper particles into many pieces. The plastic deformation of substrate materials then enlarged the cracks and caused the movement of particle fragments to form the intertwining structure. Because the plastic deformation in the first-layer coating is much higher than in the coating-substrate interfacial region as shown in Fig. 9 and 10, copper fracture tended to happen from the middle of the first-layer coating. In the case of high coating deposition efficiency (or high particle impact velocity), as shown in Fig. 11b, coating grows rapidly, and the number of rebound particles decreased simultaneously. In this case, despite the impact energy is high, the number of particles that hit on the thin-layer coating reduced dramatically. Therefore, there is no sufficient motive force to trigger the shot-peening effect and the consequent intertwining interface.

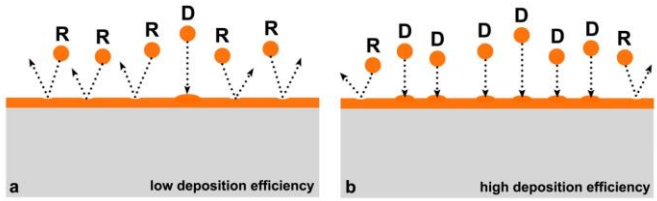

Figure 11: Schematic of the particle deposition and rebound phenomenon during coating deposition. 'D' and 'R' represent deposition particles and rebound particles, respectively

In previous works, intertwining interface was always believed to promote the interfacial bonding strength due to the intertwining structure [18]. However, the current study demonstrated that intertwining interface only generated under low particle impact velocity at which coating overall quality is low (i.e., low bonding strength, high porosity) [27,28]. In addition, the potential micro-cracks and stress concentration in the first-layer coating due to the shot-peening effect further deteriorates the coating quality. Therefore, the appearance of intertwining interface may not be a positive sign for the overall coating quality.

Conclusions

Targeted experiments and numerical simulation of cold sprayed copper onto aluminum were conducted to explore the inducing conditions and formation mechanism of intertwining interface. Experimental results showed that intertwining interface only generated at the condition of low deposition efficiency (or low particle impact velocity). Therefore, the appearance of intertwining interface may not be a positive sign for the overall coating quality. Also, prominent intertwining structures can be found beneath an extremely thin single-layer coating and further particle deposition posed negligible effect, which suggests that intertwining interface actually generated at the very beginning of coating deposition. Modeling results revealed that impact-induced plastic deformation at the intertwining interface was much stronger when the coating had only single or double layers, even at low particle impact velocity. Based on the experimental and numerical analysis, the formation mechanism of intertwining interface was concluded as follows. Low deposition efficiency lead to slow coating growing rate. Therefore, at the beginning of the coating deposition, a large number of rebound particles repetitively hit the very thin single-layer or double-layer coating, forming a shot-peening effect. Such effect resulted in periodic shear stress and plastic strain in the first-layer coating. Particles of the first-layer coating were elongated and fractured and mixed with the substrate material to form the intertwining structure. The novel findings in the present work were further confirmed by the validating experiment of copper coating onto magnesium substrate.

Acknowledgements

The authors would like to thank the financial support from Irish Research Council project (GOIPD-2017-912) and Enterprise Ireland (CF20144626).

References

[1] A. Papyrin, Cold Spray Technology, Adv. Mater. Process. 159 (2001) 49–51.

[2] H. Assadi, F. Gärtner, T. Stoltenhoff, H. Kreye, Bonding mechanism in cold gas spraying, Acta Mater. 51 (2003) 4379–4394.

[3] G. Bae, Y. Xiong, S. Kumar, K. Kang, C. Lee, General aspects of interface bonding in kinetic sprayed coatings, Acta Mater. 56 (2008) 4858–4868.

[4] X.-T. Luo, C.-X. Li, F.-L. Shang, G.-J. Yang, Y.-Y. Wang, C.-J. Li, High velocity impact induced microstructure evolution during deposition of cold spray coatings: A review, Surf. Coatings Technol. 254 (2014) 11–20.

[5] C. Lee, J. Kim, Microstructure of Kinetic Spray Coatings: A Review, J. Therm. Spray Technol. 24 (2015) 592–610.

[6] P.C. King, G. Bae, S.H. Zahiri, M. Jahedi, C. Lee, An experimental and finite element study of cold spray copper impact onto two aluminum substrates, J. Therm. Spray Technol. 19 (2010) 620–634. [7] T. Klassen, H. Assadi, H. Kreye, F. G, Cold spraying e A materials perspective, Acta Mater. 116 (2016) 382–407. doi:10.1016/j.actamat.2016.06.034.

[8] S. Yin, Y. Xie, J. Cizek, E. Ekoi, T. Hussain, D. Dowling, R. Lupoi, Advanced diamond-reinforced metal matrix composites via cold spray: Properties and deposition mechanism, Compos. Part B Eng. 113 (2017) 44–54.

[9] Q. Wang, D. Qiu, Y. Xiong, N. Birbilis, M.X. Zhang, High resolution microstructure characterization of the interface between cold sprayed Al coating and Mg alloy substrate, Appl. Surf. Sci. 289 (2014) 366–369.

[10] Q. Wang, N. Birbilis, M.X. Zhang, Interfacial structure between particles in an aluminum deposit produced by cold spray, Mater. Lett. 65 (2011) 1576–1578.

[11] K.H.H. Ko, J.O.O. Choi, H. Lee, Y.K.K. Seo, S.P.P. Jung, S.S.S. Yu, Cold spray induced amorphization at the interface between Fe coatings and Al substrate, Mater. Lett. 149 (2015) 40–42.

[12] Y.Y. Zhang, J.S. Zhang, Recrystallization in the particles interfacial region of the cold-sprayed aluminum coating: Strain-induced boundary migration, Mater. Lett. 65 (2011) 1856–1858.

[13] Y. Xiong, K. Kang, G. Bae, S. Yoon, C. Lee, Dynamic amorphization and recrystallization of metals in kinetic spray process, Appl. Phys. Lett. 92 (2008) 144–147.

[14] K. Kim, M. Watanabe, K. Mitsuishi, K. Iakoubovskii, S. Kuroda, Impact bonding and rebounding between kinetically sprayed titanium particle and steel substrate revealed by high-resolution electron microscopy, J. Phys. D. Appl. Phys. 42 (2009) 65304.

[15] S. Yin, Y. Xie, X. Suo, H. Liao, X. Wang, Interfacial bonding features of Ni coating on Al substrate with different surface pretreatments in cold spray, Mater. Lett. 138 (2015) 143–147.

[16] T. Hussain, D.G. McCartney, P.H. Shipway, D. Zhang, Bonding mechanisms in cold spraying: The contributions of metallurgical and mechanical components, J. Therm. Spray Technol. 18 (2009) 364–379.

[17] V.K. Champagne, D. Helfritch, P. Leyman, S. Grendahl, B. Klotz, Interface Material Mixing Formed by the Deposition of Copper on Aluminum by Means of the Cold Spray Process, J. Therm. Spray Technol. 14 (2005) 330–334.

[18] L. Ajdelsztajn, B. Jodoin, G.E. Kim, J.M. Schoenung, Cold spray deposition of nanocrystalline aluminum alloys, Metall. Mater. Trans. A Phys. Metall. Mater. Sci. 36 (2005) 657–666.

[19] X.L. Zhou, a. F. Chen, J.C. Liu, X.K. Wu, J.S. Zhang, Preparation of metallic coatings on polymer matrix composites by cold spray, Surf. Coatings Technol. 206 (2011) 132–136.

[20] C. Stenson, K.A. McDonnell, S. Yin, B. Aldwell, M. Meyer, D.P. Dowling, R. Lupoi, Cold spray deposition to prevent fouling of polymer surfaces, Surf. Eng. 844 (2016) 1–11.

[21] R. Liang, A.S. Khan, A critical review of experimental results and constitutive models for BCC and FCC metals over a wide range of strain rates and temperatures, Int. J. Plast. 15 (1999) 963–980.
[22] S. Yin, X.F. Wang, W.Y. Li, H.E. Jie, Effect of substrate hardness on the deformation behavior of subsequently incident particles in cold spraying, Appl. Surf. Sci. 257 (2011) 7560–7565.
[23] H. Assadi, T. Schmidt, H. Richter, J.O. Kliemann, K. Binder, F. Gärtner, T. Klassen, H. Kreye, On parameter selection in cold spraying, J. Therm. Spray Technol. 20 (2011) 1161–1176.
[24] S. Yin, M. Meyer, W. Li, H. Liao, R. Lupoi, Gas Flow, Particle Acceleration, and Heat Transfer in Cold Spray: A review, J. Therm. Spray Technol. 25 (2016) 1–23.
[25] S. Guetta, M.H. Berger, F. Borit, V. Guipont, M. Jeandin, M. Boustie, Y. Ichikawa, K. Sakaguchi, K. Ogawa, Influence of particle velocity on adhesion of cold-sprayed splats, J. Therm. Spray Technol. 18 (2009) 331–342.
[26] S. Yin, X. Wang, X. Suo, H. Liao, Z. Guo, W. Li, C. Coddet, Deposition behavior of thermally softened copper particles in cold spraying, Acta Mater. 61 (2013) 5105–5118.
[27] J. Ajaja, D. Goldbaum, R.R. Chromik, Characterization of Ti cold spray coatings by indentation methods, Acta Astronaut. 69 (2011) 923–928.
[28] R. Huang, W. Ma, H. Fukanuma, Development of ultra-strong adhesive strength coatings using cold spray, Surf. Coatings Technol. 258 (2014) 832–841.